nature immunology

SUPPLEMENTARY INFORMATION

https://doi.org/10.1038/s41590-018-0162-7

In the format provided by the authors and unedited.

TCRs are randomly distributed on the plasma membrane of resting antigen-experienced T cells

Benedikt Rossboth[1], Andreas M. Arnold[1], Haisen Ta[2], René Platzer[3], Florian Kellner[3], Johannes B. Huppa[3], Mario Brameshuber[1*], Florian Baumgart[1*] and Gerhard J. Schütz[1*]

[1]Institute of Applied Physics, TU Wien, Vienna, Austria. [2]Department of NanoBiophotonics, Max Planck Institute for Biophysical Chemistry, Göttingen, Germany. [3]Institute for Hygiene and Applied Immunology, Center for Pathophysiology, Infectiology and Immunology, Medical University of Vienna, Vienna, Austria. *e-mail: brameshuber@iap.tuwien.ac.at; baumgart@iap.tuwien.ac.at; schuetz@iap.tuwien.ac.at

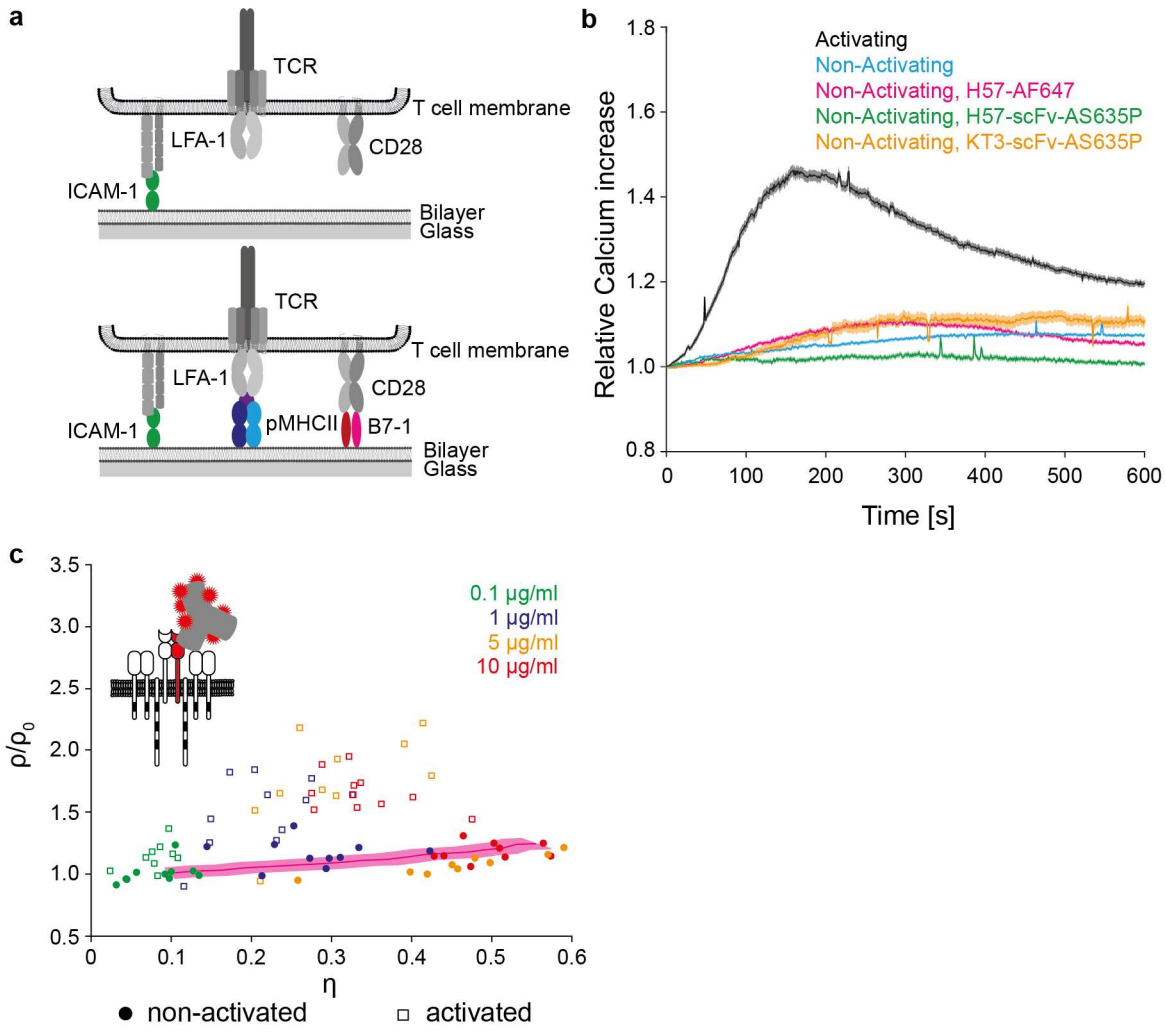

Supplementary Figure 1

T cell activation model systems, quantification of T cell activation by ratiometric Ca^{2+} imaging and titration steps in label-density-variation dSTORM with H57-AF647

(**a**) Schematic of model system: primary murine $CD4^+$ T_{EFF} cells on supported lipid bilayers displaying ICAM-1 (green) for non-activating conditions (*top*), or ICAM-1, B7-1 (*red*), and cognate pMHCII (here MCC–I-E^k) (blue) for activating conditions (*bottom*). (**b**) Ratiometric Ca^{2+} imaging via Fura-2 to assess activation state of primary murine $CD4^+$ T_{EFF} cells. T cell activation and concomitant increase in cytosolic Ca^{2+} under activating conditions (*black,* 2,128 cells from 7 independent experiments) or non-activating conditions (see **a**): unlabeled cells (*blue,* 2,362 cells from 7 independent experiments), or cells labeled with H57-AF647 (*magenta,* 763 cells from 2 independent experiments), H57-scFv-AS635P (*green,* 293 cells from 3 independent experiments), or KT3-scFv-AS635P (*orange,* 1205 cells from 4 independent experiments). Data shown as medians ± SE of the median. (**c**) Label-density-variation dSTORM using H57-AF647. Data represent one titration experiment shown in **Fig. 2b** with each data point color-coded according the antibody concentrations used for labeling; Red line and pink shading indicate the reference line and its uncertainty for a random distribution derived from simulations based on the experimentally determined blinking statistics of H57-AF647 (mean ± SEM; n=50 independent simulations).

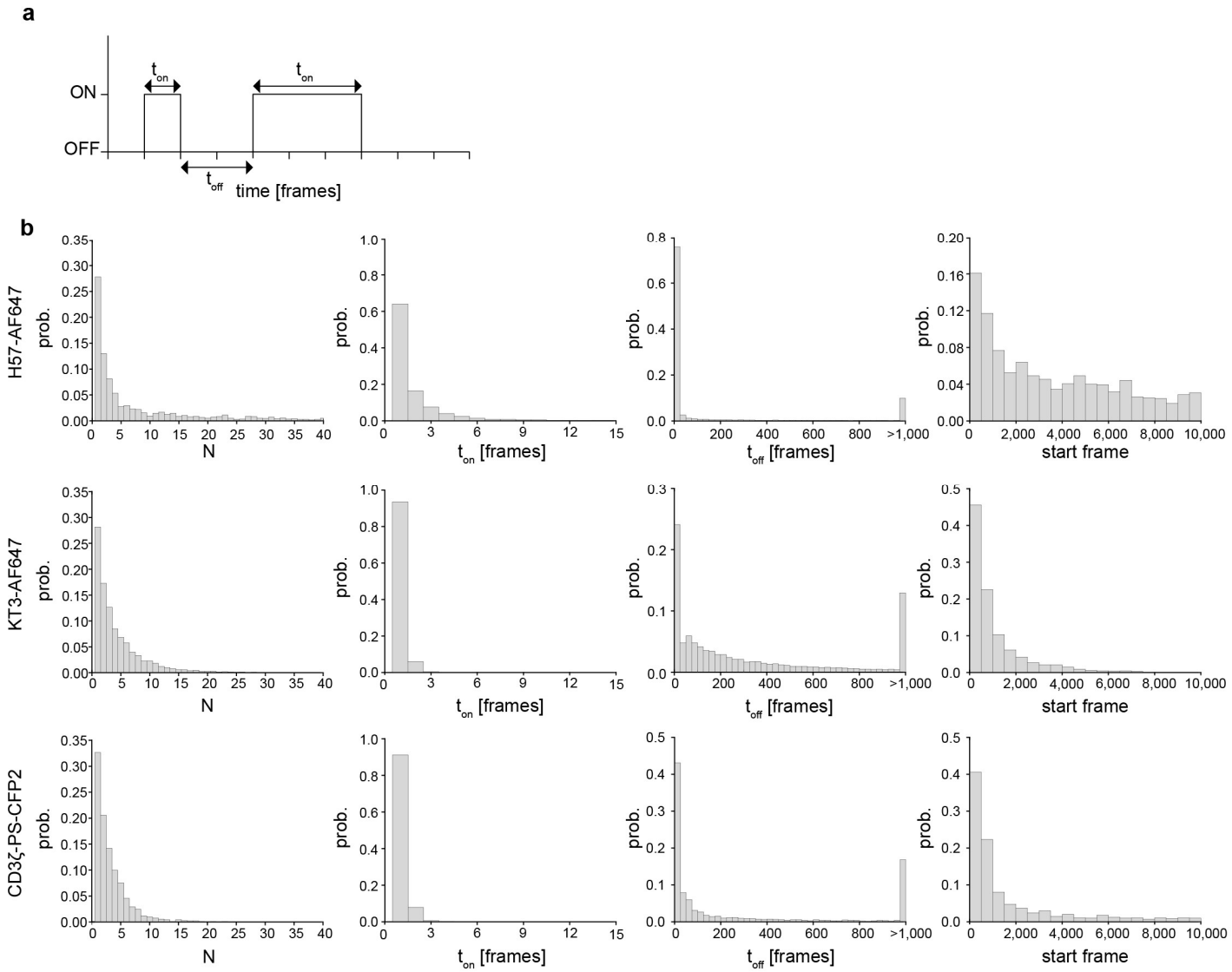

Supplementary Figure 2

Single molecule blinking statistics

Blinking statistics of labels used for label-density-variation SMLM experiments derived from time traces of recorded localizations. Data were recorded on fixed primary murine CD4$^+$ T_{EFF} cells labeled with antibody concentrations or PS-CFP2 expression levels so low that well-separated single molecule signals could be observed. (**a**) t_{on}: time a single molecule was detectable in consecutive frames, t_{off}: time a molecule remained in a dark state. (**b**) Histograms summarizing the blinking data with respect to the total number of observation per molecule, N, t_{on}, t_{off} and the first frame in which a molecule was detected; n=1,827 for H57-AF647, n=6,151 for KT3-AF647 and n=1,409 for PS-CFP2.

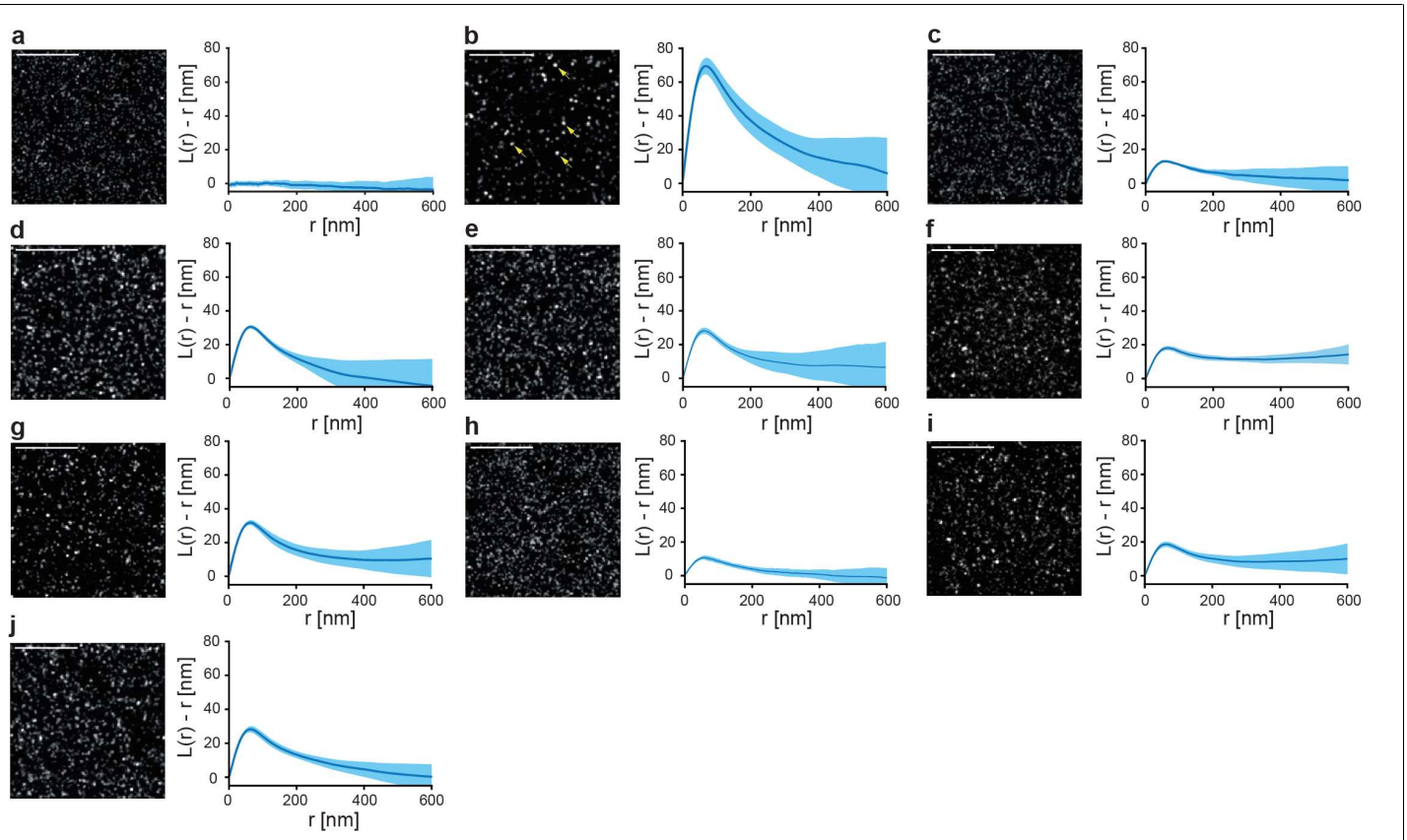

Supplementary Figure 3

Effect of blinking on SMLM data and Ripley's K analysis

A molecular density of 70 molecules/µm² in ROIs of 5 x 5 µm was simulated in 10 independent runs per condition. Blinking was simulated based on experimentally determined blinking statistics (**Supplementary Fig. 2**). Localization maps are shown for each condition (*left panels*) with corresponding Ripley's K analysis (*right panels*). Random molecular distributions were simulated (**a**) without blinking, i.e. each molecule is represented by one localization or (**b**) including blinking statistics determined for anti-TCRβ H57-AF647. Yellow arrows indicate clearly visible blinking-related localization clusters. (**c-j**) Further scenarios relevant for this study were simulated as follows: (**c**) Randomly distributed dimers without blinking; (**d**) randomly distributed dimers with blinking based on anti-CD3ε KT3-AF647; (**e**) randomly distributed dimers with blinking based on PS-CFP2; (**f**) randomly distributed dimers that diffuse according to parameters determined for the TCR (mobile fraction of 64% and D = 0.047 µm²/s) with blinking based on PS-CFP2; (**g**) randomly distributed monomers with blinking based on PS-CFP2; (**h**) a mix of 70% randomly distributed dimers and 30% randomly distributed monomers without blinking; (**i**) a randomly distributed mix of 70% dimers and 30% monomers that both diffuse according to parameters determined for the TCR (mobile fraction of 64% and D = 0.047 µm²/s) and that both show blinking based on PS-CFP2; (**j**) a randomly distributed mix of 70% dimers and 30% monomers that both show blinking based on PS-CFP2. Ripley's K curves are shown as mean ± SD; Scale bars: 2 µm.

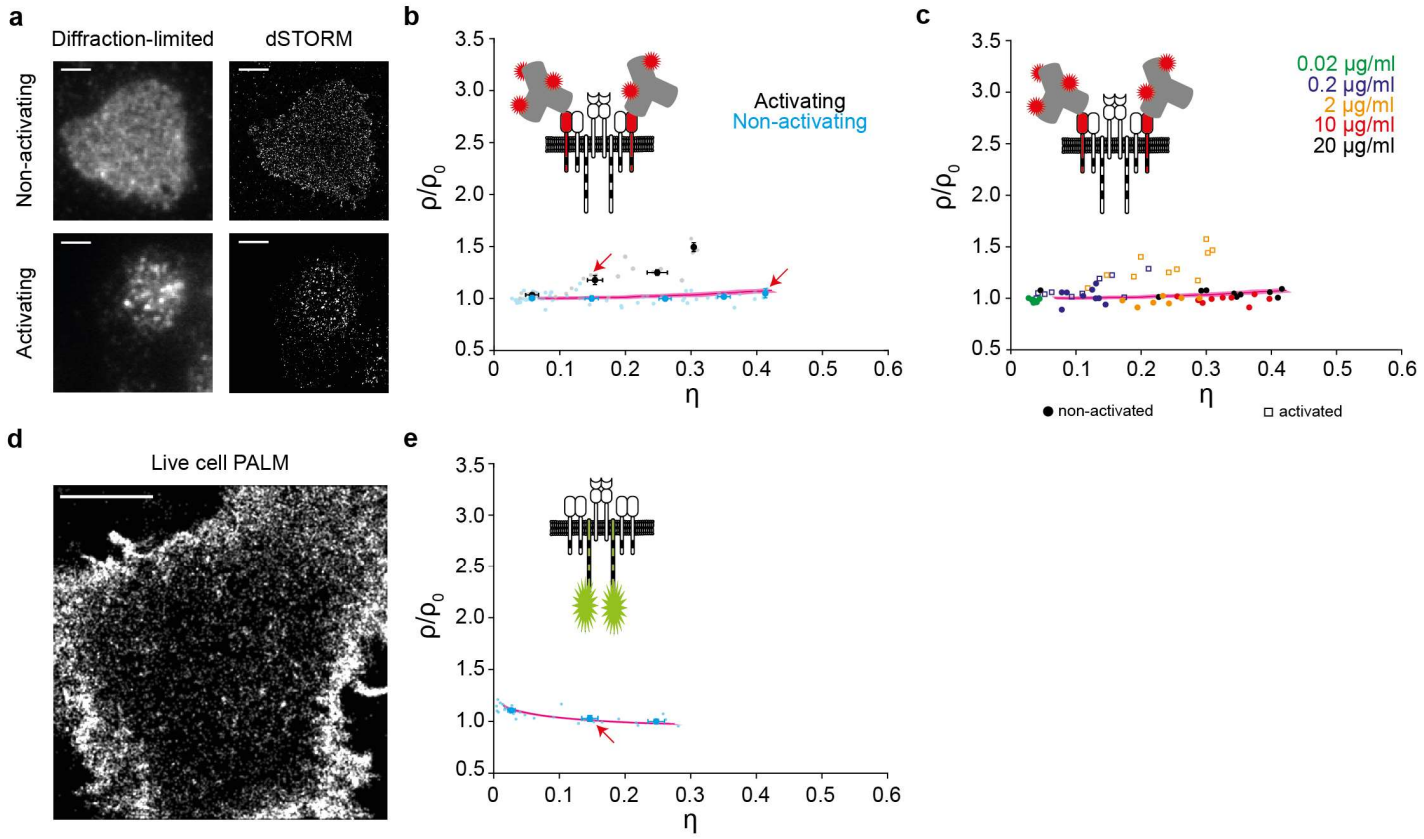

Supplementary Figure 4

Label-density-variation SMLM of CD3ε labeled with KT3-AF647 and CD3ζ-PS-CFP2

(**a**) Representative diffraction-limited microscopy images (*left*) and dSTORM localization maps (*right*) of fixed primary murine CD4⁺ T_{EFF} cells labeled with KT3-AF647 during interaction with non-activating (*top*) or activating (*bottom*) supported lipid bilayers (n=10 and n=19 biologically independent samples for activating and non-activating conditions, respectively); Scale bars: 3 µm. (**b**) Normalized ρ-versus-η plot derived from label-density-variation dSTORM of fixed primary mouse CD4+ TEFF cells under non-activating or activating conditions (key) labeled with KT3-AF647 (0.02, 0.2, 2 and 20 µg/ml): red arrows indicate data points corresponding to the cells in **a**; inset (top left), labeling strategy. Each symbol (gray or blue shading) represents an individual cell (n = 58 samples (non-activating) or n = 20 samples (activating)); red line and pink shading indicate the reference line and its uncertainty, respectively, for a random distribution derived from simulations based on the experimentally determined blinking statistics of KT3-AF647 (mean ± s.e.m. of n = 50 independent simulations). Data were binned from four independent experiments based on η with a bin size of 0.1 and represented as mean ± s.e.m: blue (non-activating), black (activating). (**c**) Label-density-variation dSTORM using KT3-AF647. Data are identical to **b** with each data point color-coded according the antibody concentrations used for labeling; red line and pink shading indicate the reference line and its uncertainty for a random distribution derived from simulations based on the experimentally determined blinking statistics of KT3-AF647 (mean ± SEM; n=50 independent simulations). (**d**) Live primary murine CD4⁺ T_{EFF} expressing CD3ζ-PS-CFP2 under non-activating conditions. Representative map of all recorded localizations is shown (n=29 biologically independent samples. Scale bars: 3 µm. (**e**) Normalized ρ versus η plot derived from label density variation PALM based on the intrinsic expression level variabilities of primary murine CD4⁺ T_{EFF} cells expressing CD3ζ-PS-CFP2 under non-activating conditions (key): red arrows indicate data points corresponding to the cell in **d**; inset (top left), labeling strategy. Each symbol (blue shading) represents an individual cell (n = 29 samples); red line and pink shading indicate the reference line and its uncertainty, respectively, for a random distribution derived from simulations based on the experimentally determined blinking statistics of PS-CFP2 (mean ± s.e.m. of n = 50 independent simulations). Data were binned from two independent experiments based on η with a bin size of 0.1 and represented as mean ± s.e.m (blue).

.

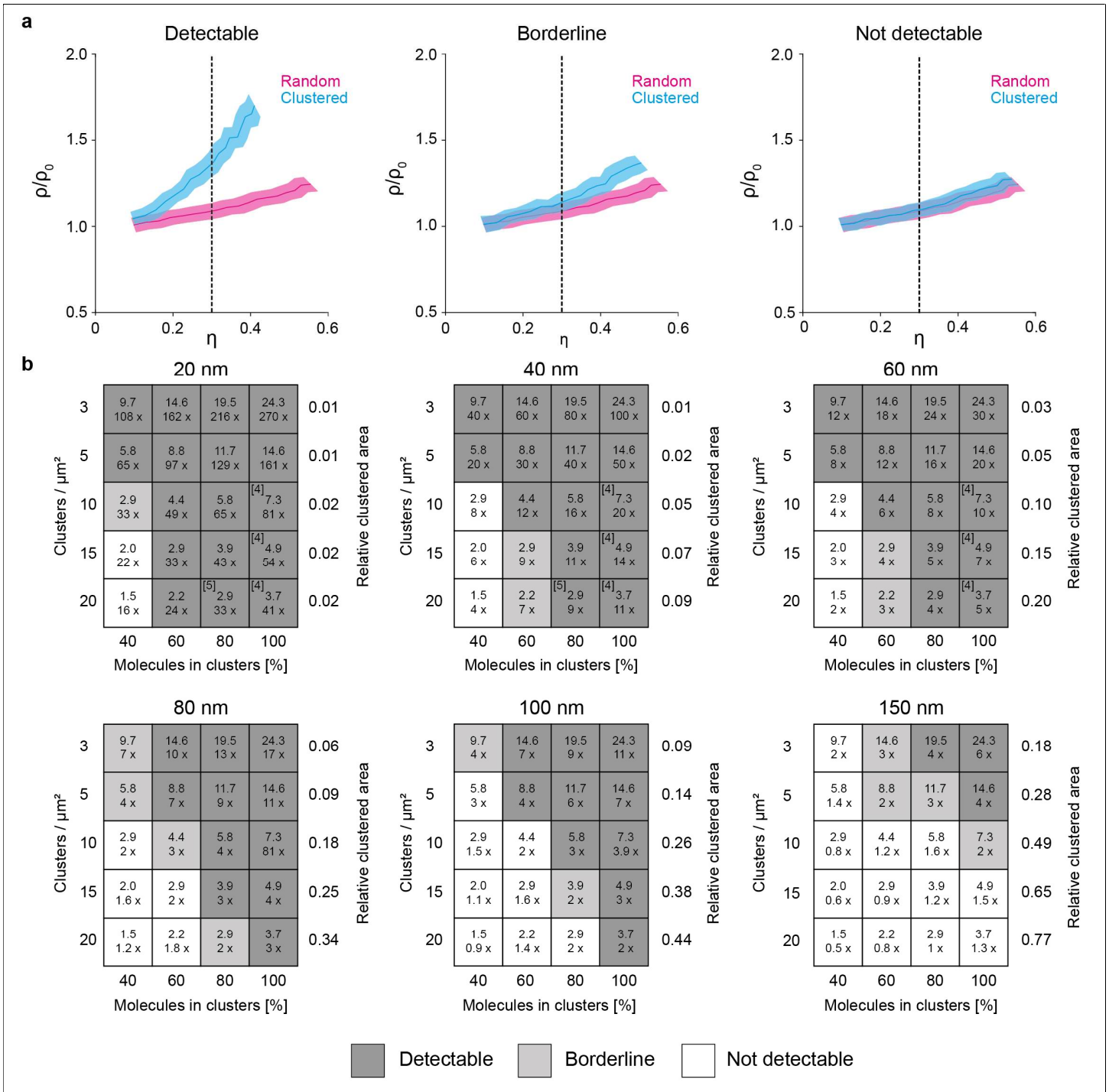

Supplementary Figure 5

Classification criteria for cluster detection and sensitivity of label-density-variation SMLM to detect nanoclustering in experiments using H57-AF647

(**a**) Schematic normalized ρ versus η plots of random (*red*) and different cluster scenarios (*blue*): cluster scenarios were classified as clearly detectable, when confidence intervals did not show overlap at η=0.3 (*left*); as borderline, when confidence intervals overlapped at η=0.3, but mean values were outside the confidence intervals (*center*); as not detectable, when mean values were lying within the

respective confidence intervals at η=0.3 (*right*). All curves are plotted as mean ± SEM. The dashed line indicates η=0.3, where the detectability was evaluated. (**b**) Normalized ρ versus η plots were calculated for different simulated clustering scenarios and assessed for the difference from simulated random molecular distributions; detectable difference (dark gray), borderline (light gray) and not detectable difference (white) as shown in **a**. Reference numbers indicate scenarios published in the literature. Simulations of nanoclusters with radii of 20, 40, 60, 80, 100 and 150 nm for 3, 5, 10, 15 and 20 clusters/μm². The fraction of molecules inside clusters was varied between 40% and 100%. Average molecular densities were adjusted to 73 molecules/μm² based on H57-AF647 labeling of TCRβ (**Fig. 2a**). Blinking statistics were based on experimental data of H57-AF647. Numbers in boxes indicate the average number of molecules per cluster and the relative enrichment of molecules inside *versus* outside of clusters is indicated. The relative clustered area (*right*) was calculated from thresholded binary cluster maps. The figure is an extension of **Fig. 4a**: panels for 20 nm and 60 nm are identical to **Fig. 4a**.

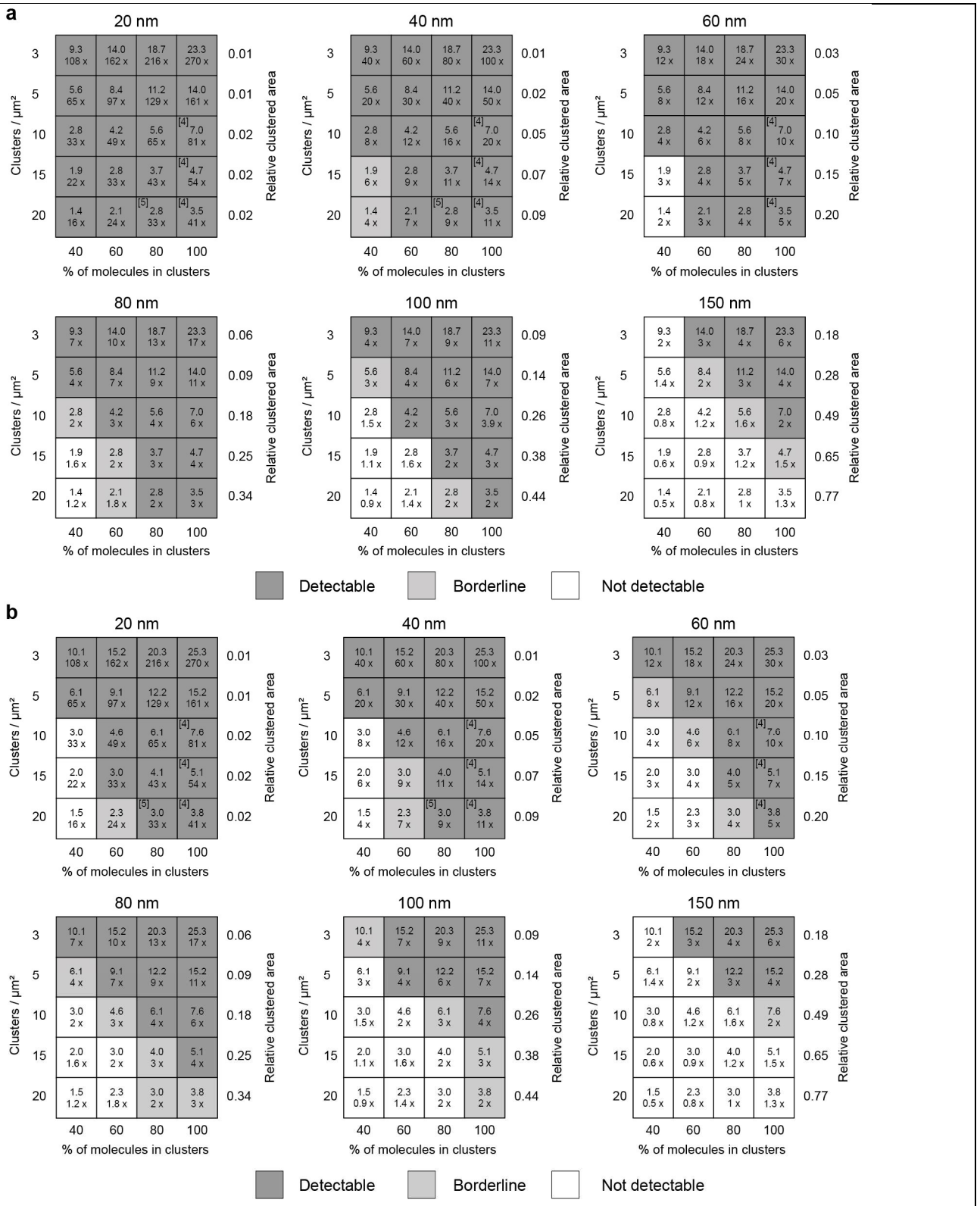
a
20 nm
40 nm
60 nm
80 nm
100 nm
150 nm
Clusters / µm²
Relative clustered area
% of molecules in clusters
Detectable
Borderline
Not detectable
b
20 nm
40 nm
60 nm
80 nm
100 nm
150 nm
Clusters / µm²
Relative clustered area
% of molecules in clusters
Detectable
Borderline
Not detectable

Supplementary Figure 6

Sensitivity of label-density-variation SMLM to detect nanoclustering in experiments using KT3-AF647 (a) and PS-CFP2 (b)

Normalized ρ versus η plots were calculated for different simulated clustering scenarios and assessed for the difference from simulated random molecular distributions; detectable difference (dark gray), borderline (light gray) and not detectable difference (white) (see **Supplementary Fig. 5a**). Reference numbers indicate scenarios published in the literature. Simulations of nanoclusters with radii of 20, 40, 60, 80, 100 and 150 nm for 3, 5, 10, 15 and 20 clusters/µm². The fraction of molecules inside clusters was varied between 40% and 100%. Average molecular densities were adjusted to (**a**) 70 molecules/µm² based on KT3-AF647 labeling of CD3ε (**Supplementary Fig. 5a**) or (**b**) 76 molecules/µm² based on ζ-PS-CFP2 PALM experiments (**Fig. 3a**). Blinking statistics were based on experimental data of the respective fluorescent probes. Numbers in boxes indicate the average number of molecules per cluster and the relative enrichment of molecules inside *versus* outside of clusters is indicated. The relative clustered area (*right*) was calculated from thresholded binary cluster maps. **b** is an extension of **Fig 4b:** panels for 20 nm and 60 nm are identical to **Fig. 4b**.

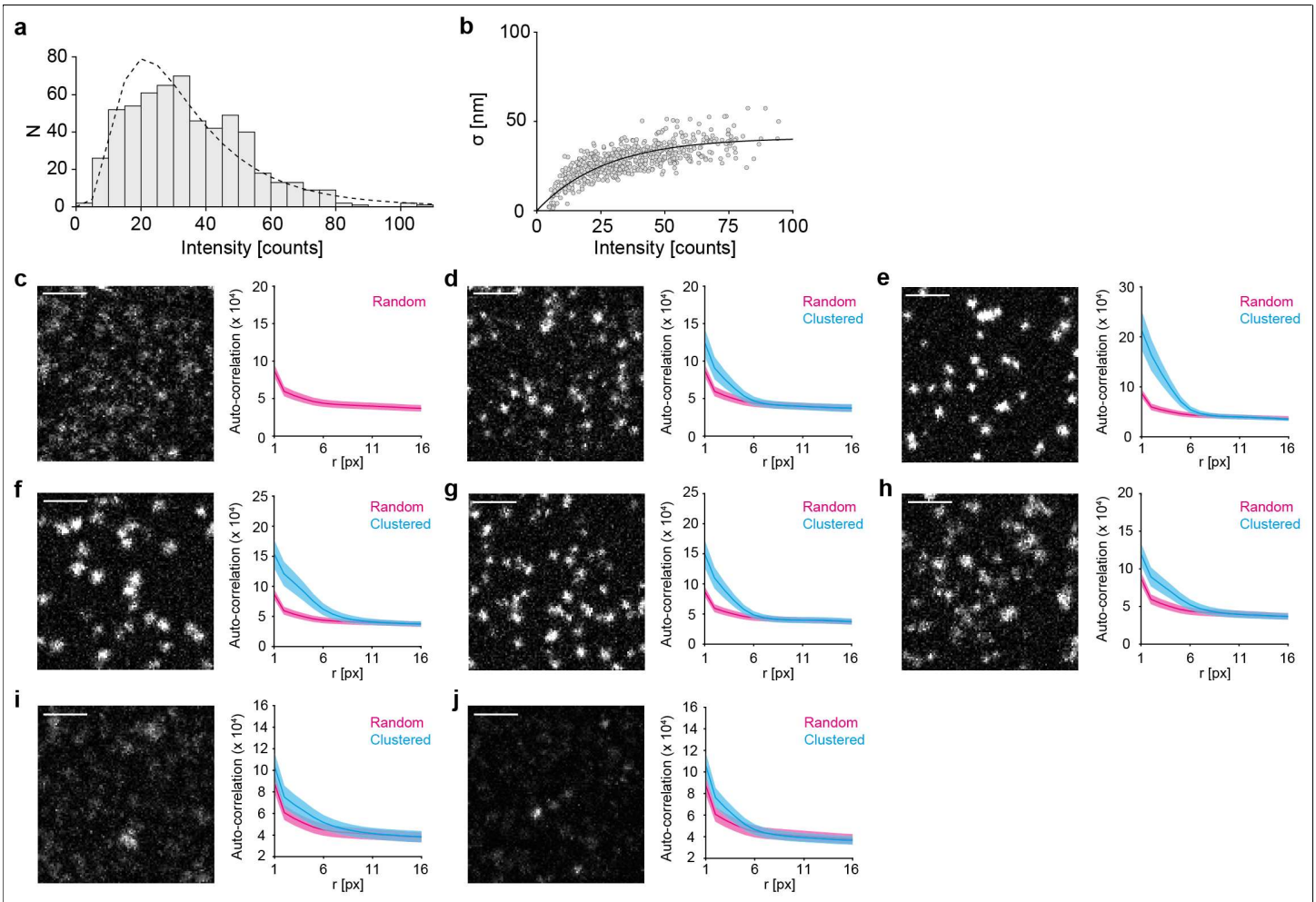

Supplementary Figure 7

Characterization of single molecule signals in STED microscopy and simulated STED microscopy data of different clustering scenarios

Characterization of single molecule signals in STED microscopy: (**a**) Fitting of single molecule signals with a Gaussian intensity profile yielded the integrated intensity (*I*) and the width (σ). Values for *I* could be fitted well with a log-normal distribution (dashed line), yielding a mean of 35.14 and a variance of 508.52. (**b**) The signal width σ showed a characteristic dependence on the intensity. The data were fitted with Eq. 1 (black line).

Simulated STED microscopy images (left) analyzed by image autocorrelation analysis. Red curves represent analysis of simulated random data (n=5); blue curves represent analysis of simulated cluster scenarios (n=5). Molecular densities were matched to the experiment. (**c**) A random distribution of molecules. (**d-j**) Different cluster scenarios characterized by cluster radius (r), fraction of molecules inside clusters and density of clusters per area (clusters/µm²): (**d**) r=20 nm, 80% in clusters, 20 clusters/µm²; (**e**) r=20 nm, 100% in clusters, 10 clusters/µm²; (**f**) r=60 nm, 100% in clusters, 10 clusters/µm²; (**g**) r=20 nm, 100% in clusters, 20 clusters/µm²; (**h**) r=60 nm, 100% in clusters, 20 clusters/µm²; (**i**) r=100 nm, 15% in clusters, 0.5 clusters/µm²; (**j**) r=40 nm, 10% in clusters, 0.5 clusters/µm². Curves are shown as means ± SEM; Scale bars: 500 nm.

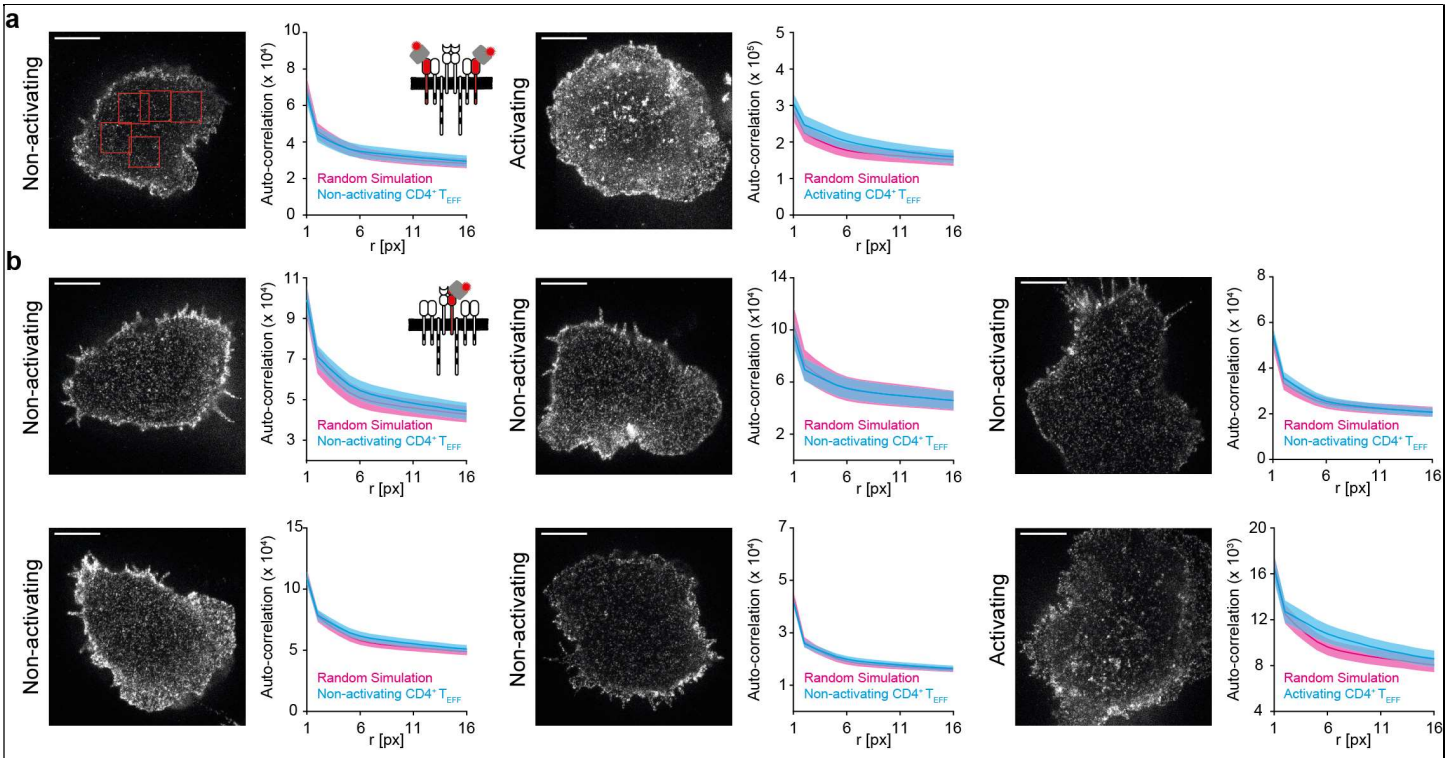

Supplementary Figure 8

STED microscopy of TCRβ or CD3ε and image autocorrelation analysis

Representative STED microscopy images of fixed primary murine CD4⁺ T_{EFF} cells labeled with (**a**) KT3-scFv-AS635P (n = 2 biologically independent samples for both activating and non-activating conditions) or (**b**) H57-scFv-AS635P during interaction with non-activating or activating supported lipid bilayers as indicated (n=5 and n=1 biologically independent samples for non-activating and for activating conditions, respectively); Recorded images (left) were analyzed by image autocorrelation (right) and compared to simulated random distributions at molecular densities matched to the experimental data. Red curves represent simulated random data (mean ± SEM.; n=5); blue curves represent analysis of multiple ROIs in the respective images (mean ± SEM.; n=5). Red boxes in STED images indicate ROI positions chosen for ACF analysis. ROI positions were chosen similarly in other images (not shown). Scale bars: 3 µm; Cartoons illustrate the labeling strategy.

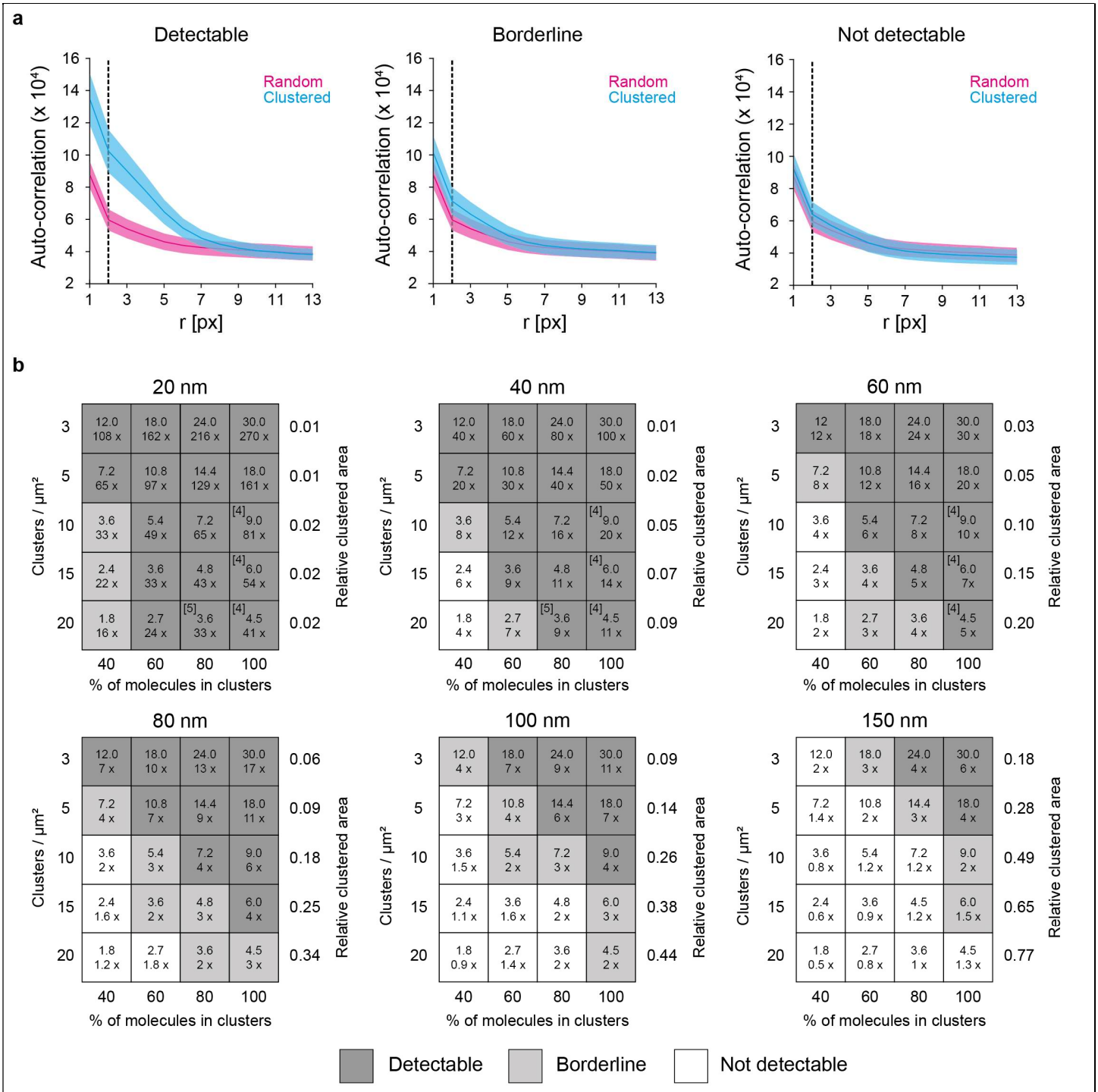

Supplementary Figure 9

Classification criteria for cluster detection and sensitivity of STED image autocorrelation analysis to detect nanoclustering

(**a**) Schematic of image autocorrelation curves of random (*red*) and different cluster scenarios (*blue*): cluster scenarios were classified as clearly detectable, when confidence intervals did not show overlap within the first two data points (*left*); as borderline, when confidence intervals overlapped within the first two data points, but mean values were outside the confidence intervals (*center*); as not detectable, when mean values were lying within the respective confidence intervals within the first two data points (*right*). All curves are plotted as

mean ± SEM. The dashed line indicates that detectability was evaluated within the first two data points. (**b**) Image autocorrelation analysis was performed for different simulated clustering scenarios and assessed for the difference from simulated random molecular distributions; detectable difference (dark gray), borderline (light gray) and not detectable difference (white) as shown in **a**. Reference numbers indicate scenarios published in the literature. Simulations of nanoclusters with radii of 20, 40, 60, 80, 100 and 150 nm for 3, 5, 10, 15 and 20 clusters/µm². The fraction of molecules inside clusters was varied between 40% and 100%. Average molecular densities were adjusted to 75 molecules/µm² based on KT3-scFv-AS635P labeling of CD3ε (**Fig. 5**). Parameters of the simulated point spread function were based on experimental data. Numbers in boxes indicate the average number of molecules per cluster and the relative enrichment of molecules inside *versus* outside of clusters is indicated. The relative clustered area (*right*) was calculated from thresholded binary cluster maps. The figure is an extension of **Fig. 6**: panels for 20 nm and 60 nm are identical to **Fig. 6**.